Environmental Science Advances

ROYAL SOCIETY OF CHEMISTRY

PAPER

View Article Online
View Journal | View Issue

Check for updates

Cite this: *Environ. Sci.: Adv.*, 2023, **2**, 313

Hemocompatibility of biogenic phosphorus nano-agromaterials at environmentally relevant and supra-environmental concentrations for occupational exposure†

Ayushi Priyam,[ab] Luis O. B. Afonso,[b] Aaron G. Schultz,[b] Amit Kumar Dinda[c] and Pushplata Prasad Singh*[ab]

Phosphorus (P)-based nanomaterials (NMs), such as those derived from rock phosphate (RP) and hydroxyapatite (HAP), have the potential to be used as nanofertilisers to supplement depleting P levels in agricultural soils. Before applying to agricultural areas, complete profiling is essential to assess the potential risk to human health from occupational exposure, particularly for the predicted environmentally relevant concentration (ERC) magnitudes. A systematic investigation on blood contact properties such as percent hemolysis, platelet aggregation, blood coagulation time, and interactions with serum plasma protein was performed in this *ex vivo* study using National Institute of Health (NIH) guidelines. For ERCs (0–50 μg mL^{-1}) and supra-environmental concentrations (SECs, 50–1000 μg mL^{-1}), the effects of biologically synthesised nanohydroxyapatite (nHAP) and nanophosphorus (nP) were compared to those of chemically synthesised and commercially available nHAPs and bulk RP. Our results show that biogenic nHAP and nP did not have any significant effect on hemolysis, platelet aggregation or coagulation processes at ERCs and SECs whereas the bulk RP had significant hemotoxic effects. Protein quantification analysis revealed that proteins from blood serum adsorb onto NMs, forming a biomolecular corona. Our results highlight the hemocompatible behaviour of biologically synthesized P-based NMs at predicted ERCs, which are most likely to be occupational exposures. These findings may provide a fundamental understanding of the overall risks presented by P-based nanofertilisers.

Received 1st October 2022
Accepted 7th December 2022

DOI: 10.1039/d2va00237j

rsc.li/esadvances

Environmental significance

Phosphorus-based nanomaterials (NMs) are being explored for their use as fertilisers to improve agricultural productivity. However, there is limited information on the interactions between such nanofertilisers and human blood. Also, there is a key knowledge gap about the subsequent impact of such interactions on the biotransformation and human safety of nanofertilisers. This work reports that the biosynthesised P-based NMs were more hemocompatible than the bulk analogues that are traditionally used in agriculture. This study demonstrates the interaction between P-based NMs and blood components and provides important evidence for their human risk assessment.

1 Introduction

Nanomaterials (NMs) are now widely used in a variety of fields, including consumer goods, science, engineering, medicine, and agriculture, owing to their higher surface area-to-volume ratios, which result in increased efficacy.[1] Phosphorus (P) deficiency occurs in agricultural soils all over the world as a result of limited natural availability and mismanagement in current agricultural practices.[2] Bulk P fertilisers derived from rock phosphate (RP), diammonium phosphate (DAP), or tricalcium phosphate (TCP) are commonly used to meet agricultural demands.[3] Bulk P fertilisers have limitations due to poor plant uptake and run-off into water bodies, resulting in terrestrial and aquatic contamination.[3] As a result, P-based NMs are intended for agricultural use.[4] At the research scale, apatite-based NMs, more commonly known as nanohydroxyapatite (nHAP), are being investigated for use as nanofertilisers.[5–7] Nano-phosphorus (nP), a nanoscale derivative of RP with improved uptake efficiency and efficacy, has also been proposed as a P-supplementing fertiliser.[7–9]

[a]*National Centre of Excellence for Advanced Research in Agricultural Nanotechnology, TERI – Deakin Nanobiotechnology Centre, Sustainable Agriculture Division, The Energy and Resources Institute (TERI), DS Block, India Habitat Centre, Lodhi Road, New Delhi, 110003, India. E-mail: pushplata.singh@teri.res.in*

[b]*School of Life and Environmental Sciences, Deakin University, Geelong, Victoria, 3217, Australia*

[c]*Department of Pathology, All India Institute of Medical Sciences, Ansari Nagar, New Delhi, 110029, India*

† Electronic supplementary information (ESI) available. See DOI: https://doi.org/10.1039/d2va00237j

Open Access Article. Published on 20 prosince 2022. Downloaded on 27.01.2026 16:22:53. This article is licensed under a Creative Commons Attribution-NonCommercial 3.0 Unported Licence.

Open Access Article. Published on 20 prosince 2022. Downloaded on 27.01.2026 16:22:53.
This article is licensed under a Creative Commons Attribution-NonCommercial 3.0 Unported Licence.

Given the differences in the properties and behaviour of bulk and nano forms, many international regulatory agencies have made human and environmental safety assessments mandatory prior to the commercialization of agriculturally relevant NMs. A better understanding of the potential risk of NMs necessitates an assessment of their potential hazard to human and environmental receptors at varying exposure concentrations. The magnitudes of exposure depend on applied NM concentrations, environmentally relevant concentrations (ERCs) and supra-environmental concentrations (SECs) accumulated over long periods of time, following multiple applications and NM transformation.[10,11] As a bone material, HAP is considered biocompatible.[12] However, nanoscale conversion frequently results in the development of novel physicochemical properties in the parent material, which may alter the NM biocompatible behaviour.[13] Further, to develop P-based NMs, strong alkaline and acidic conditions are used during chemical synthesis.[14] Chemical wastes generated during synthesis contribute to environmental pollution furthermore.[14] A general hypothesis suggests that using a green or biogenic method instead of toxic chemicals may improve eco-compatibility at NM synthesis levels,[15–17] though a complete safety profiling of the biogenic NMs is also required before their applications. Occupational exposure to farmers may occur if nHAP and nP are used as fertilisers. This direct occupational exposure is hypothesised to occur at applied NM concentrations; however, a reasonable chance of indirect exposure after NM application remains at other ERCs and SECs. Following applications, NMs can interact with humans in either pristine or environmentally transformed forms. Environmental transformations of these agriculturally useful NMs may happen after they interact with factors such as organic (*e.g.* humic acid and enzymes secreted by microbes) and inorganic (various ions, *e.g.* Fe^{3+} and Al^{3+}) components in soil, temperature and UV from the sun.[18,19] Such factors may result in eco-corona over the NMs and influence their indirect exposure to humans.[19]

Because of their small size, these NMs can enter the circulatory system through dermal contact or inhalation in both direct and indirect exposure. One of the most important factors to consider for the evaluation of the potential hazard of such applied NMs is their hemocompatibility profiling. The Nanoparticle Characterization Laboratory (NCL, USA) protocol cascade and ISO-10993-4 recommend testing for hemolysis, coagulation, platelets, hematology and the complement system to understand the potential risk from NM interaction with blood.[20]

When NMs enter the circulatory system, they come into contact with blood cells as well as plasma proteins, which might modulate or trigger pathophysiologic processes. The coordinated interaction of endothelium, platelets and coagulation factors in the vascular compartment ensures the maintenance of vascular and tissue homeostasis. The presence of P-based NMs in the vascular environment may affect this homeostasis dynamic by interacting with endothelial cells, platelets and coagulation factors. As a result, assessing nHAP and nP NMs in this context is a critical requirement for their safety profile. The biocompatibility of nHAP has been studied, with a focus on bone tissue[21,22] but there is little information on its interaction with the vascular compartment.[21,23] The current state of reports on the biological effects of nHAP on blood lacks a comprehensive analysis of thorough NM characterization and defining the biological effects in accordance with physicochemical properties. As a result, conclusions about the biocompatible size or shape of P-based NMs vary greatly.[21,23–26] So far, effects of chemically synthesized nHAPs have been reported only for *in vitro* hemolysis. Furthermore, including a relevant bulk source as one of the experimental controls to compare the effects of NMs is critical but has not been thoroughly investigated. This will help in drawing comparisons on the hemocompatibility of NMs in order to supplement their use as fertilisers. As a result, the blood compatibility of variously shaped P-based NMs must be thoroughly investigated. The effect of biogenic P-based NMs on human blood is reported in this study. We conducted a systematic investigation of hemolysis, platelet aggregation, coagulation and interaction with plasma protein after treatment with different synthesised and shaped nHAP and nP and evaluated effects at ERCs and SECs.

2 Materials and methods

All experiments were performed strictly in accordance with relevant guidelines and regulations by the Nanoparticle Characterization Laboratory, National Cancer Institute, National Institute of Health, USA. The experiments were ethically approved by Deakin University, Australia.

2.1. Materials

Potassium ferricyanide, potassium cyanide, potassium dihydrogen phosphate, Triton X 100, calcium chloride, Tris base, SDS, Bradford reagent, collagen and hydroxyapatite nanopowder (product no. 677418, size < 200 nm, spherical shaped) were procured from Sigma-Aldrich (USA). Another hydroxyapatite nanopowder (product no. 13616, size < 200 nm, needle shaped) was procured from Sisco Research Laboratories Pvt. Ltd. (India). Dulbecco's phosphate buffer saline (DPBS) was procured from Gibco, Thermofisher Scientific (USA).

2.2. Nanomaterial samples

Biologically synthesized nHAP (Ca/P ratio as 1.583, size 35.74 nm, platelet shaped) and chemically synthesized nHAP (Ca/P ratio as 1.79, size 83.92 ± 26.85 nm, rod shaped) were synthesized in-house using previously published methods.[17] Both of these NMs have also been thoroughly characterized in our previous study using transmission electron microscopy, dynamic light scattering, FTIR and XRD.[17] In brief, the biologically synthesized nHAP was platelet shaped, with a size of 35.74 nm, Ca/P ratio of 1.583, and a hydrodynamic diameter of 325.8 ± 37.1 nm and zeta potential of −31.3 ± 3.5 mV in MilliQ water (ESI Table 1†). In contrast, the chemically synthesized nHAP was rod shaped, with a size of 83.92 ± 26.85 nm, Ca/P ratio of 1.79, and a hydrodynamic diameter of 756.2 ± 28.8 nm and zeta potential of −45.2 ± 1.7 mV in MilliQ water (ESI Table 1†). Nanophosphorus (nP) nanoparticles were kindly

 © 2023 The Author(s). Published by the Royal Society of Chemistry

Open Access Article. Published on 20 prosince 2022. Downloaded on 27.01.2026 16:22:53.
This article is licensed under a Creative Commons Attribution-NonCommercial 3.0 Unported Licence.

provided by the TERI-Deakin Nanobiotechnology Centre, Gurugram, India, for this study. The particles of nP were spherical shaped, with a size of ~5–10 nm, Ca/P ratio of ~3.8, and hydrodynamic diameter of 798.5 ± 23.36 nm and zeta potential of −11.61 ± 0.015 mV in MilliQ water (ESI, Table 1†). The NMs alongside with bulk controls RP and Ca_3PO_4 were used at the following concentrations in different assays unless stated otherwise: 0, 1.5625, 3.125, 6.25, 12.5, 25, 50, 100, 200, 500 and 1000 μg mL^{-1}.

2.3. Human blood samples

Blood samples in this study were collected from healthy volunteers after taking written informed consent. The study followed the recommendations made in the declaration of Helsinki and the blood samples were used in accordance with the institutional human ethics approval (DUHREC reference no. 2021-095: Deakin University Human Research Ethics Committee, Australia).

2.4. Hemolysis assay

The hemolysis assay was carried out according to the protocol from the National Cancer Institute (NCI).[20] Briefly, for the analysis whole blood was required where the level of plasma free hemoglobin (PFH) concentration was below 1 mg mL^{-1}. Pooled blood obtained from healthy donors was diluted with 1× DPBS (Dulbecco's PBS) to adjust total blood hemoglobin (TBH) concentration to 10 ± 2 mg mL^{-1} (TBHd). 100 μL of 1× DPBS as negative control, nHAPs and nP solutions (concentrations mentioned in Section 2.2) in 1× DPBS as test samples and Triton-X-100 as positive control were added to 96-well plates. 100 μL of TBHd was added to each well and the plate was incubated at 37 °C for 3 h. The plate was then centrifuged at 800 × *g* for 15 min. 100 μL supernatant and 100 μL cyanmethemoglobin (CMH) reagent[20,27] were added to a fresh 96-well plate. The absorbance (OD) at 540 nm was determined by the H1 hybrid microplate reader (Biotek, USA). For each term of the equation, the OD value was already subtracted by their background interference. The assay threshold is 20% platelet aggregation for acceptable blood compatible materials. For the result acceptance, the % coefficient of variance for each sample was within 20%. The percentage of hemolysis was calculated using the equation:

$$\%\ \text{hemolysis} = \text{hemoglobin in sample/TBHd} \times 100.$$

2.5. Blood cell aggregation assay

Platelet-rich plasma (PRP) was obtained by pooling fresh human plasma from at least three donors by centrifugation at 200 × *g* for 8 min. 25 μL of nHAP and nP solution diluted by 1× DPBS, 1× DPBS as negative control or 1 mg mL^{-1} collagen (Sigma-Aldrich, USA) as positive control were mixed with 100 μL PRP, respectively. Then, all samples – NMs and bulk (concentrations mentioned in Section 2.2) were incubated at 37 °C for 15 min. The cell counting (CC) was performed by using a hemocytometer. Individual cells were counted to get the final cell count. The percentage of blood cell aggregation was calculated using the equation:

$$\%\ \text{blood cell aggregation} = (CC_{\text{negative control}} - CC_{\text{sample}})/(CC_{\text{negative control}}) \times 100\%.$$

2.6. Blood coagulation time

Blood was collected from healthy voluntary donors with informed consent, in heparinized vials. 50 μL of NMs and bulk samples at different concentrations (concentrations mentioned in Section 2.2) were incubated with 50 μL of blood for 5 minutes at room temperature. 25 μL of 50 mM calcium chloride was added to it and mixed gently.[28,29] Time was noted from the addition of NMs to the first visible sign of a clot.

2.7. Blood protein binding – corona over nanoparticles

To investigate the formation of plasma protein corona on nHAP and nP, the presence of adsorbed protein was quantified using Bradford's method and FTIR. 1 mg mL^{-1} of nHAPs and nP were incubated for 3 h at room temperature with plasma in 1 (sample) : 3 (plasma) ratio by volume. The samples were centrifuged for 30 min at 15 000 rpm, 4 °C. Pellets were washed with 1× PBS for three times. The washes were kept for soft corona analysis. The last pellets were dispersed in 1× PBS for hard corona analysis. Protein in washes and hard corona was quantified using Bradford's method[30] and samples were checked for the presence of amide and carboxylic functional groups using FTIR (Nicolet 6700, Thermo Fisher Scientific, USA).

2.8. Statistical analysis

Statistical analysis was performed using Graphpad Prism (v8.4). All values were expressed as mean ± standard deviation (S.D.) of samples ($n = 3$) in a representative experiment. For each of the NMs (nHAPs and nP), we characterized dose–effect relationships with human blood. The data was checked for normal distribution using Shapiro–Wilk test and the normal distribution of residuals was checked on QQ plots. The effects on hemolysis, blood cell aggregation and plasma coagulation time were subjected to ANOVA to check if the variance was significant. This would not explicitly tell where the significant differences lie and were, thus, then followed by a Tukey *post hoc* multiple comparison test, to identify the treatment groups with a significant difference in mean values. A *p*-value less than 0.05 was considered as statistically significant.

3 Results

3.1. Blood contact properties of nHAPs and nP in terms of hemolysis, blood cell aggregation and blood coagulation time

For different test materials including the nHAPs, nP, bulk sources RP and Ca_3PO_4, negative and positive controls, the values of % hemolysis (Fig. 1), % blood cell aggregation (Fig. 2)

Open Access Article. Published on 20 prosince 2022. Downloaded on 27.01.2026 16:22:53.
This article is licensed under a Creative Commons Attribution-NonCommercial 3.0 Unported Licence.

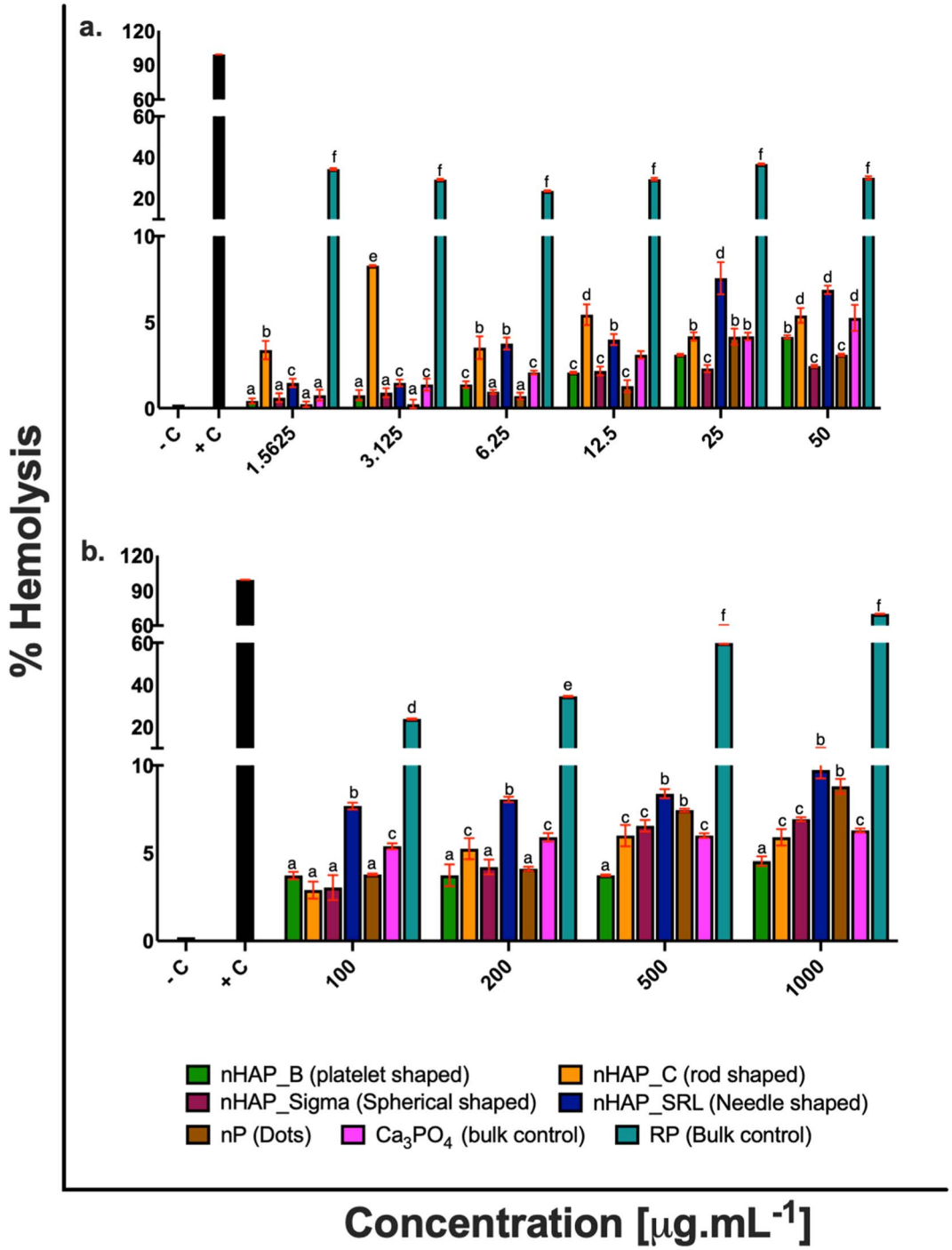

Fig. 1 Hemolysis after treatment with (a) environmentally relevant concentrations (1.5625, 3.125, 6.25, 12.5, 25 and 50 μg mL^{-1}) and (b) higher applied concentrations (100, 200, 500 and 1000 μg mL^{-1}) of biologically synthesized nHAP (nHAP_B), chemically synthesized nHAP (nHAP_C), Sigma-Aldrich nHAP (nHAP_Sigma), SRL nHAP (nHAP_SRL), nanophosphorus (nP), rock phosphate bulk control (RP), and calcium phosphate bulk control (Ca_3PO_4). Controls: 0.1% (v/v) Triton X 100 as a positive control (+C) and 1× DPBS as negative control (−C). Values reported as mean ± S.D. [Different letters denote statistically significant differences between the test samples ($p < 0.05$)].

and blood coagulation time (Fig. 3) are presented in Table 1 at highest tested ERC (50 μg mL^{-1}) and SEC (1000 μg mL^{-1}). It was found that the P-based NMs did not cause any toxicity with reference to the key blood contact parameters with LC_{50} expected to be beyond the highest tested SEC in each case. To further understand if the type of these P-based NMs (shape and synthesis) influences their behavior with blood cells and the consequent effects, statistical analyses were conducted. Each NM was compared with every other NM for % hemolysis (ESI Table 2†), % blood cell aggregation (ESI Table 3†) and blood

© 2023 The Author(s). Published by the Royal Society of Chemistry

Open Access Article. Published on 20 prosince 2022. Downloaded on 27.01.2026 16:22:53.
This article is licensed under a Creative Commons Attribution-NonCommercial 3.0 Unported Licence.

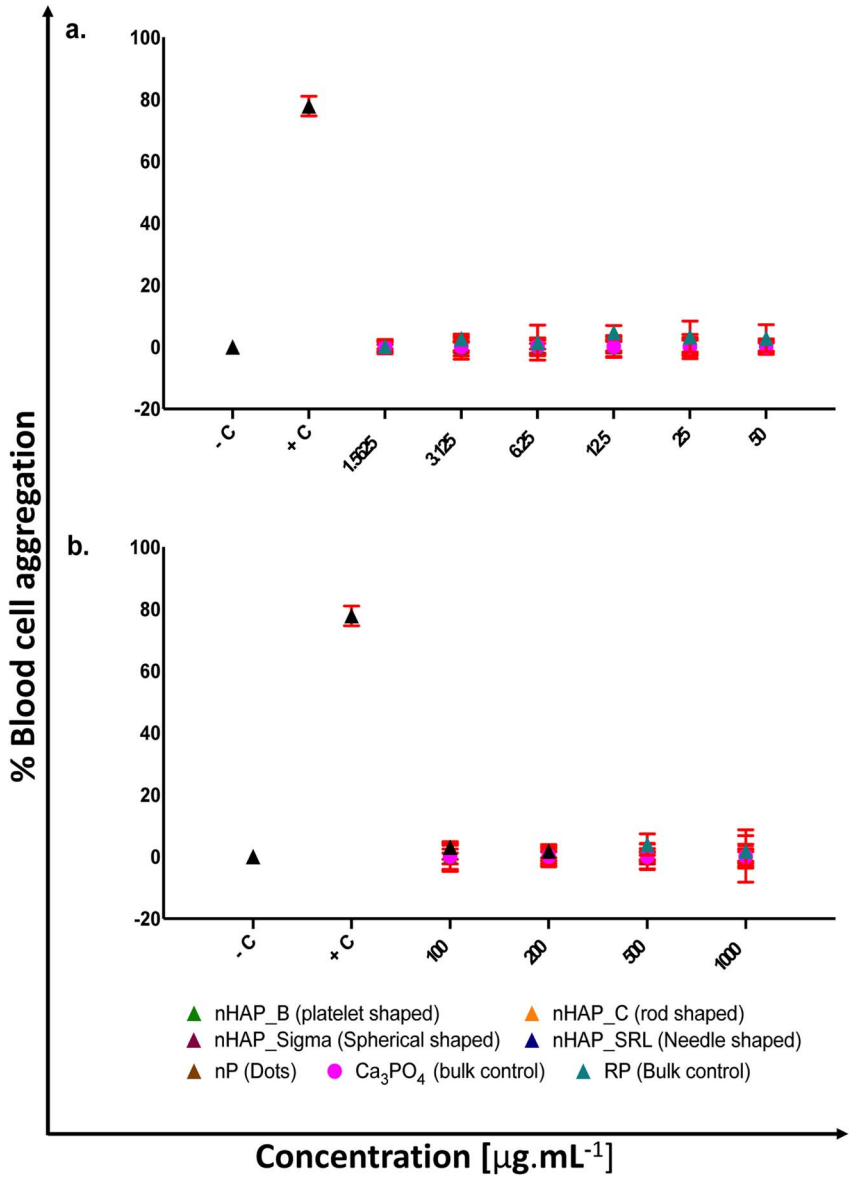

Fig. 2 % blood cell aggregation after treatment with (a) environmentally relevant concentrations (1.5625, 3.125, 6.25, 12.5, 25 and 50 μg mL^{-1}) and (b) higher applied concentrations (100, 200, 500 and 1000 μg mL^{-1}) of biologically synthesized nHAP (nHAP_B), chemically synthesized nHAP (nHAP_C), Sigma-Aldrich nHAP (nHAP_Sigma), SRL nHAP (nHAP_SRL), nanophosphorus (nP), rock phosphate bulk control (RP), and calcium phosphate bulk control (Ca_3PO_4). Controls: 1 $mg.mL^{-1}$ collagen as a positive control (+C) and 1× DPBS as negative control (−C). Values reported as mean ± S.D.

coagulation time (ESI Table 4†) using a two-way ANOVA followed by Tukey *post hoc* test for $p < 0.05$.

nHAP_B and nHAP_Sigma were found to be significantly more hemocompatible as compared to nHAP_C (rod-shaped) and nHAP_SRL (needle-shaped) (ESI Fig. 1†). nP (dots) was significantly more hemocompatible in comparison to its bulk source RP (ESI Fig. 1†). RP was found to be highly hemolytic at all the tested concentrations. Statistically significant ($p < 0.05$) differences in overall hemolytic trend were found between platelet, rod, spherical shaped and dots of P-based NMs. Shape-dependent differences in NM uptake into a cell could have elicited different pathways to draw out the observed pattern of hemolysis.

There was no significant acceleration of platelet aggregation in the case of treatments with different nHAPs and nP at environmentally relevant concentrations, *i.e.* up to 50 μg mL^{-1} (Fig. 2a). The overall effect on aggregation due to the shape and synthesis route was assessed statistically (ESI Fig. 2†). It was found that blood cell aggregation was not significantly affected by different shapes and differently synthesized nHAPs.

There was a slight increase in blood coagulation time when the blood cells were exposed to different concentrations of nHAPs and nP. However, both at the highest tested ERC and SEC, the values were found in the range for physiological activated partial thromboplastin time (APTT is between 25.1 and 36.5 s).[31–33] Also, a follow-up from ANOVA using Tukey's *post hoc*

Open Access Article. Published on 20 prosince 2022. Downloaded on 27.01.2026 16:22:53.
This article is licensed under a Creative Commons Attribution-NonCommercial 3.0 Unported Licence.

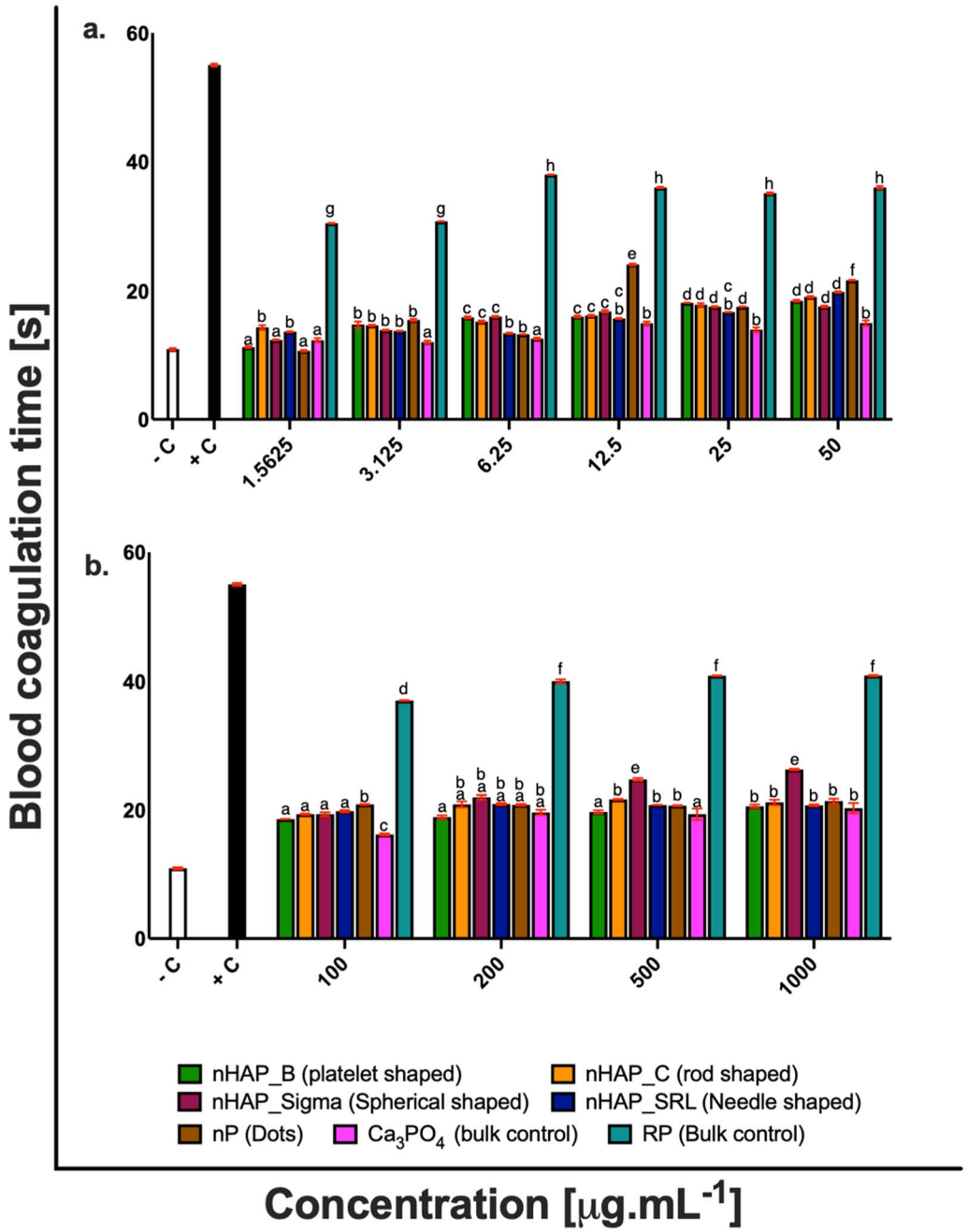

Fig. 3 Blood coagulation time after treatment with (a) environmentally relevant concentrations (1.5625, 3.125, 6.25, 12.5, 25 and 50 μg mL^{-1}) and (b) higher applied concentrations (100, 200, 500 and 1000 μg mL^{-1}) of biologically synthesized nHAP (nHAP_B), chemically synthesized nHAP (nHAP_C), Sigma-Aldrich nHAP (nHAP_Sigma), SRL nHAP (nHAP_SRL), nanophosphorus (nP), rock phosphate bulk control (RP), and calcium phosphate bulk control (Ca_3PO_4). Controls: 50 mM $CaCl_2$ as a positive control (+C) and 1× DPBS as negative control (−C). Values reported as mean ± S.D. [Different letters denote statistically significant differences between the test samples ($p < 0.05$)].

analysis revealed that the overall effect of different concentrations of nHAP_B on blood coagulation time was significantly different from nHAP_C, nHAP_Sigma, nHAP_SRL, nP and the bulk sources (ESI Fig. 3†).

3.2. Protein corona over nanoparticles

The results from Bradford's assay (Fig. 4) show that only a small concentration of protein forms a hard corona on the surface of NPs and most of the proteins form a soft corona and get washed off. Essentially in a hard corona, by quantification it was found that the protein concentrations were 0.28 ± 0.05, 0.24 ± 0.01, 0.35 ± 0.10, 0.23 ± 0.01 and 0.32 ± 0.11 mg mL^{-1}, respectively, for nHAP_B (platelet-shaped), nHAP_C (rod-shaped), nHAP_-Sigma (spherical), nHAP_SRL (needle-shaped) and nP (dots). From Fig. 4, it could be observed that for hard corona proteins, there was a slight increase in protein concentrations for

 © 2023 The Author(s). Published by the Royal Society of Chemistry

Open Access Article. Published on 20 prosince 2022. Downloaded on 27.01.2026 16:22:53.
This article is licensed under a Creative Commons Attribution-NonCommercial 3.0 Unported Licence.

Table 1 Values for hemolysis, blood cell aggregation and blood coagulation time for different test materials at the highest tested ERC and SEC. Data presented as mean ± standard deviation ($n = 3$)

	% hemolysis		% blood cell aggregation		Blood coagulation time [s]	
	ERC (50 μg mL^{-1})	SEC (1000 μg mL^{-1})	ERC (50 μg mL^{-1})	SEC (1000 μg mL^{-1})	ERC (50 μg mL^{-1})	SEC (1000 μg mL^{-1})
Negative control	0.21 ± 0.001%		0		10.9 ± 0.16	
Positive control	99.18 ± 0.08%		77.87 ± 0.55%		55 ± 0.21	
nHAP_B	4.13 ± 0.1%	4.5 ± 0.26%	0.15 ± 0.44%	0.15 ± 0.56%	18.4 ± 0.14	20.6 ± 0.28
nHAP_C	5.38 ± 0.43%	5.9 ± 0.46%	0.20 ± 0.28%	0.20 ± 0.66%	19.05 ± 0.12	21.19 ± 0.41
nHAP_Sigma	2.43 ± 0.07%	6.9 ± 0.11%	0.18 ± 0.31%	0.19 ± 0.40%	17.6 ± 0.11	26.26 ± 0.10
nHAP_SRL	6.88 ± 0.25%	9.7 ± 0.49%	0.20 ± 0.23%	0.17 ± 0.26%	19.8 ± 0.11	20.73 ± 0.14
nP	3.09 ± 0.07%	8.8 ± 0.42%	0.18 ± 0.38%	0.29 ± 1.46%	21.7 ± 0.07	21.4 ± 0.36
RP	29.98 ± 0.82%	69.99 ± 0.21%	2.87 ± 0.76%	1.89 ± 0.85%	36 ± 0.22	40.88 ± 0.08
Ca_3PO_4	5.24 ± 0.76%	6.29 ± 0.11%	0.15 ± 0.43%	0.20 ± 0.38%	14.97 ± 0.44	20.29 ± 0.30

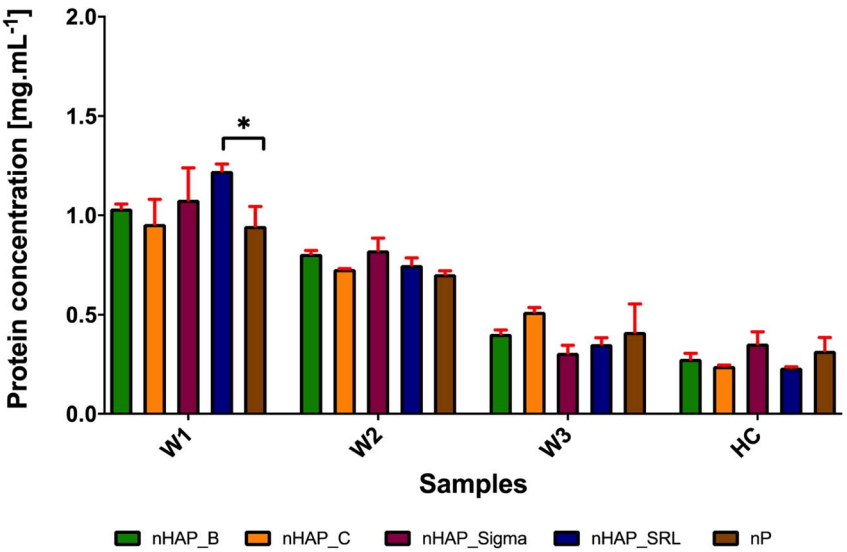

Fig. 4 Protein quantification of corona on biologically synthesized nHAP (nHAP_B), chemically synthesized nHAP (nHAP_C), Sigma-Aldrich nHAP (nHAP_Sigma), SRL nHAP (nHAP_SRL) and nanophosphorus (nP) due to interaction with blood serum plasma. W1, W2, W3 and HC denote proteins in wash 1, wash 2, wash 3 and hard corona, respectively. Significance denoted as: * for $p < 0.05$ between the first wash of nHAP_SRL and nP.

spherical shaped nHAP_Sigma and dots of nP. The statistically significant differences between W1, W2, W3 and HC in the case of all the NMs are presented in ESI Table 2.† Also, a qualitative FTIR analysis of hard corona for these nanoparticles (ESI Fig. 4†) showed the presence of peaks for amide C=O stretch, carboxylic acid OH stretch and amide N–H stretch, respectively, at 1650, 2360–2370 and 3270–3380 cm^{-1}. The presence of these peaks suggests that the P-based NMs may develop protein capping in the form of the hard corona that contains the presence of peptide bonds, which remains intact after rigorous washings.

4 Discussion

Environmental risks of NMs are assessed by characterizing their exposure levels and corresponding biological effects in terrestrial and aquatic environments. Due to the lack of information from direct measurements, ERCs and SECs are estimated from exposure modelling. Their potential effect on biological species is measured under controlled experimental conditions using a range of applied NM concentrations. The gap between *in vitro* experiments and real conditions may influence the environmental relevance of current risk assessments and exposure models, including test conditions, bioavailable concentrations, mode of action, NM production volumes, transformations, trophic transfers and model validation. Identifying the realistic environmentally relevant concentrations of NMs is difficult due to such analytical barriers.[34] Thus, NMs are used in laboratory conditions often at concentrations higher than the expected NM concentrations in the environment.[35] Identification of ERCs for NM is critical to study its overall fate and risk. A more general approach to evaluate NM compatibility has been to study the toxic endpoints after exposures that are far more than those relevant to realistic environmental scenarios to have an overall dose-dependent safety analysis.

© 2023 The Author(s). Published by the Royal Society of Chemistry

Open Access Article. Published on 20 prosince 2022. Downloaded on 27.01.2026 16:22:53.
This article is licensed under a Creative Commons Attribution-NonCommercial 3.0 Unported Licence.

Holden and colleagues (2014),[36] tabulated the modelled NM ERC magnitudes for two environmental compartments – water (surface or wastewater) and solid media (biosolids, soil and sediments). This typically ranged between 0.001 and 1 ppm in the case of water compartments and 0.001–1000 ppm in the case of solid media compartments for various metallic and carbonaceous NMs. The same research group evaluated the average (mode) NM ERCs as 5.1, 55.1, 550.1 and 5500.1 ppm in aquatic organisms, microorganisms, soil/sediment/wastewater and terrestrial plants, respectively. According to another study by Zhao and colleagues (2020)[37] on metallic (TiO_2, Ag, CuO) and carbonaceous (carbon nanotubes) NMs, the predicted ERCs were low and varied depending upon the presence and transfer of NMs in the water (~0 to 2×10^3 ppb), sediments (~0 to 200 ppm) and soil (2 to 4 magnitude lower than concentrations in sediments).[37] From the trends suggested above, it may be considered that concentrations between 50 and 100 ppm may be considered as ERC thresholds depending on aquatic sediments or terrestrial systems respectively. Even though P as an element is not foreign to our cells, yet the different nanoforms of P may undergo unique interactions with blood proteins and biological membranes, which may or may not be safe for cells. Based on the variation in shape-dependent effects of P-based NMs within *in vitro* human osteoblast (MC3T3) and osteosarcoma (MG63) cells,[38,39] *in vivo* among invertebrates,[38] fish and higher vertebrates,[40,41] we planned to assess the potential adverse effects on blood contact behavior at ERCs for differently shaped and synthesized P-based NMs.

The presence of NM in the bloodstream could interfere with the homeostatic balance within the vascular compartment, which is normally maintained by an interplay between endothelium, platelets and the coagulation cascade.[42,43] HAP and calcium phosphate NMs are widely used in various medical[44,45] and agricultural[46,47] applications. Despite the wide range of established and potential applications, there is a scarcity of data on their vascular compatibility. This work was set up to evaluate the dose effects of P-based NMs: nHAP and nP, focusing on the relevance of shape and synthesis routes to establish the blood biosafety profile. The effect of multiple variants of nHAPs and nP on hemocompatibility in comparison to bulk was addressed for platelet shaped and biosynthesized nHAP_B, biosynthesised dots of nP, rod-shaped and chemically synthesized nHAP_C, commercial nHAP particles – spherical shaped (nHAP_Sigma) and needle shaped (nHAP_SRL). Blood compatibility of nHAP and nP particles was evaluated for hemolysis, blood cell aggregation, and coagulation, in a broad concentration range involving both ERCs (~1–50 μg mL^{-1}) and higher applied concentrations (>50–1000 μg mL^{-1}).

Our results suggested that unlike other metallic NMs such as Ag,[33,48] Zn[49,50] and Cu,[51,52] P-based nanoformulations were more hemocompatible than their bulk source. Previous reports suggested that needle-shaped nHAP tested at 10 mg mL^{-1} in mice erythrocytes[53,54] and rod-like nHAP assayed in human erythrocytes,[55] up to 4 mg mL^{-1} were hemocompatible. However, in this study neither platelet and spherical biogenic nHAP and nP nor spherical, rod and needle-shaped chemically synthesized nHAPs affected erythrocyte integrity up to 1000 μg mL^{-1}, as the percentage of hemolysis, measured by the release of hemoglobin, was comparable to the negative control. Thus, the results from this study suggest that for various intended applications biogenic P-based NMs will be safe in terms of occupational exposure.

Additionally, on assays performed in platelet rich plasma (PRP), all the nHAPs and nP had little effect on the platelets' function. Platelets are very sensitive to changes in the blood microenvironment being activated by a number of different stimuli, such as physiological molecules (*e.g.* thrombin, collagen, immunoglobulins), microorganisms, drugs and particulate compounds.[56] Platelet activation is associated with changes in morphology, development of pseudopodia, activation of cell membrane markers and release of signaling molecules and pro-coagulant compounds, together leading to platelet aggregation.[56] nHAPs and nP induced insignificant blood cell aggregation up to 1 mg mL^{-1}. These results are in coherence with a previous study performed in rod-like nHAP.[55]

The effect of these P-based NMs on the coagulation time was also analyzed. In our study, we found that nHAPs and nP were not thrombotic and under all the tested conditions there was no significant delay in clotting time as compared to the negative control. This suggests that different nanoforms of HAPs and P do not elevate the intrinsic and extrinsic mechanisms upon interaction with blood. Blood coagulation is evaluated by both intrinsic and extrinsic mechanisms. Coagulation time can be evaluated by activated partial thromboplastin time (APTT). It has been known that the normal physiological range for APTT is between 25.1 and 36.5 s.[31–33] The blood clotting is initiated by an enzyme which converts fibrinogen to fibrin monomers called thrombin. In the normal clotting process, fibrins are transformed into fibrin threads which are the basic clot mesh. Blood coagulation is a sequence of proteolytic reactions that may get activated within the plasma by surface-mediated events (intrinsic pathway) and upon vascular/endothelial injury and the contact of blood with the sub-endothelial tissues (extrinsic pathway). Both pathways may lead to the formation of thrombin that converts soluble fibrinogen into an insoluble fibrin network that stabilizes the platelet aggregates to form a blood clot (thrombus). *In vivo*, these proteolytic reactions occur mostly on anionic phospholipid membrane surfaces, from activated platelets or endothelial cells, and require calcium as a cofactor.[33]

Besides the effect of individual NMs and bulk controls on different assays, the overall effect of the shape and synthesis route was also analyzed statistically. It was found that the shape had a key role to decide the consolidated effects on hemolysis and blood coagulation time, whereas, it may not have a significant ($p > 0.9998$) role in blood cell aggregation. Significant ($p < 0.0001$) differences were found amongst platelet, rod, needle, spherical and dot types of NMs for hemolytic potential. For blood coagulation time, the spherical and dot type NMs were not significantly different ($p > 0.9998$); however, they had significant ($p < 0.0001$) differences with respect to platelet, rod and needle types of NMs. When compared for synthesis routes, it was found that the behavior of biogenic NMs was more compatible with human blood as compared to chemical

 © 2023 The Author(s). Published by the Royal Society of Chemistry

Open Access Article. Published on 20 prosince 2022. Downloaded on 27.01.2026 16:22:53.
This article is licensed under a Creative Commons Attribution-NonCommercial 3.0 Unported Licence.

analogues with an overall effect as significant ($p < 0.0001$). Different synthesis routes could have resulted in different physicochemical properties of the same material. These properties attenuate the biological adverse effects. In this case, the overall effects of NMs on blood could be attributed to various complex interactions between the blood cells, biomolecules and the NMs, which are again dependent on the NM type. Between the bulk RP and the P-based NMs, the nanoformulations were more hemocompatible with an overall effect as significant ($p < 0.0001$) for hemolysis and blood coagulation.

We also evaluated the preliminary interaction of plasma proteins with nHAPs and nP and the formation of hard corona. The plasma constitutes approximately 55% of the total blood. Plasma contains about 90 percent water, with 10 percent being made up of ions, proteins, dissolved gases, nutrient molecules, and wastes. The proteins in plasma include the antibody proteins, coagulation factors and the proteins albumin and fibrinogen which maintain serum osmotic pressure. As checked from FTIR and Bradford assay, the preliminary protein analysis confirmed the presence of proteins on all the nHAPs and nP in this study. It was found that most of the protein was removed by washing and only a small number of proteins remained as hard corona (HC) on the surface of all NMs. The NMs of nHAP_Sigma (spherical) and nP (small dots) had more concentration of protein on the hard corona. This might suggest that the shape of P-based NMs may influence the quantity of protein adsorbed on their surface for hard corona formation. However, further investigation is required to conclude the observation made here. From FTIR, the amide and carboxylic stretch peaks confirmed bound proteins to NMs. Since the essential hemocompatibility was obtained for all the P-based NMs used in the study, we limited our study from further dwelling into detailed proteome analysis to predict biological responses. However, theoretically, corona proteins are responsible for coagulation, hemostasis, platelet or complement activation and immune responses. It has been demonstrated by Huang *et al.* (2016)[33] that corona proteins contained both promoting and counteracting effects for these biological responses. This study suggested that majorly, kininogen-1, apolipoprotein, fibrinogen alpha chain and vitronectin seem to be abundant on hard corona for negatively charged NMs. In the case of adsorption by apolipoproteins and opsonins, there is preferential uptake of NMs by endothelial cells.[33] It has been previously established that the presence of apolipoproteins modulates the immune response by facilitating the anti-inflammatory properties and inhibition of platelet aggregation *via* L-arginine nitric oxide pathway.[57,58] Additionally, the small molecular weight proteins (10–30 kDa) on NM may impart antithrombotic functions to NMs.[59] We, therefore, hypothesized that small molecular weight proteins may comprise the HC, which may not alter the hemocompatibility of these P-based NMs on interaction with whole blood. Since the particles are negatively charged, it may also be suggested that proteins with an isoelectric point (pI) greater than 7 could have participated in the formation of HC.[60,61] Many factors may affect corona composition, which includes sizes, modifications, and cores of NMs as well as molecular weight, pI, abundance, protein interactions and even structure properties of plasma proteins.[60–63] It is important to characterize the corona proteins to comment on the preferential binding of different proteins.

Our results emphasized that hematological profiling by studying the blood contact properties of NMs both at ERCs and higher applied dosages may be crucial for the prediction of the effects of P-based NMs on various bioreceptors. These effects are further modulated by the addition of biomolecules such as proteins when the NMs interact in a biological environment. Typically, on interaction with blood, serum proteins get adsorbed to the NM surface forming a hard corona. Though we quantified serum proteins, the exact biomolecule responsible for the behaviour of these surface modified NMs remained yet to be determined. Therefore, this work opens a wide scope to study the mechanism of corona formation and protein selectivity. Altogether, this study provides a systematic overview of the hemocompatibility of biogenic and chemically synthesized P-based NMs with variations in shapes and sizes.

5 Conclusions

In the present study, we investigated the potential hemocompatibility of nHAP and nP. A range of concentrations from 1 to 1000 μg mL^{-1} were tested, and it was found that biogenic nHAP and nP did not induce hemolysis in human heparinized erythrocytes at environmentally relevant concentrations (<50 μg mL^{-1}). The hemolytic indices of these NMs were comparable with the negative control. The NMs did not show any obvious effect on RBC, WBC or platelet aggregation at different tested concentrations. The coagulation process was also studied where different concentrations of the NMs did not interfere with the clotting time of whole blood. Tests with plasma protein interaction suggested that when interacting with whole blood, protein corona formed over nHAPs, and nP did not interfere with normal blood functions. From the preliminary investigation on blood compatibility, it may be concluded that the biogenic P-based NMs did not introduce any deleterious effect on human whole blood at environmentally relevant concentrations.

Author contributions

Conceiving and designing the experiments: AP, AKD, PPS. Wet-lab work and data compilation: AP. Data analyses and manuscript writing: AP and PPS. Critical inputs and finalization of the manuscript: AP, LOA, AGS, AKD and PPS.

Conflicts of interest

The authors declare the following conflict of interest: nanophosphorus (nP) is the nanomaterial developed at TERI-Deakin Nanobiotechnology Centre (TDNBC), Gurgaon, India and is to be filed with the Indian patent office for synthesis and characterization. nP is the intellectual property of TDNBC.

Open Access Article. Published on 20 prosince 2022. Downloaded on 27.01.2026 16:22:53.
This article is licensed under a Creative Commons Attribution-NonCommercial 3.0 Unported Licence.

Acknowledgements

The research activities are supported by the Department of Biotechnology, India (grant no. BT/NNT/28/SP30280). The research activities of the authors are supported by the TERI-Deakin Nanobiotechnology Centre, Gurugram, India, All India Institute of Medical Sciences, India and Deakin University, Victoria, Australia.

References

1 H. Wang, *et al.*, Multifunctional inorganic nanomaterials for energy applications, *Nanoscale*, 2020, **12**(1), 14–42.
2 A. Ditta and A. Khalid, Bio-organo-phos: a sustainable approach for managing phosphorus deficiency in agricultural soils, *Organic Fertilizers—From Basic Concepts to Applied Outcomes*, 2016, pp. 109–136.
3 S. Ding, *et al.*, Internal phosphorus loading from sediments causes seasonal nitrogen limitation for harmful algal blooms, *Sci. Total Environ.*, 2018, **625**, 872–884.
4 M. Tang, *et al.*, Highly efficient adsorption of uranium (VI) from aqueous solution by a novel adsorbent: titanium phosphate nanotubes, *Environ. Sci.: Nano*, 2018, **5**(10), 2304–2314.
5 K. Rop, *et al.*, Formulation of slow release NPK fertilizer (cellulose-graft-poly (acrylamide)/nano-hydroxyapatite/soluble fertilizer) composite and evaluating its N mineralization potential, *Ann. Agric. Sci.*, 2018, **63**(2), 163–172.
6 A. Mikhak, *et al.*, Synthetic nanozeolite/nanohydroxyapatite as a phosphorus fertilizer for German chamomile (Matricaria chamomilla L.), *Ind. Crops Prod.*, 2017, **95**, 444–452.
7 M. B. Taşkın, *et al.*, Effect of synthetic nano-hydroxyapatite as an alternative phosphorus source on growth and phosphorus nutrition of lettuce (Lactuca sativa L.) plant, *J. Plant Nutr.*, 2018, **41**(9), 1148–1154.
8 M. M. Rady, *et al.*, Integrative Application of Soil P-Solubilizing Bacteria and Foliar Nano P Improves Phaseolus vulgaris Plant Performance and Antioxidative Defense System Components under Calcareous Soil Conditions, *J. Soil Sci. Plant Nutr.*, 2019, 1–20.
9 S. Kundu, *et al.*, Enhancing N Use Efficiency and Reducing N_2O Emission by Coating Urea with Newly Identified Bio-Molecule ($C_{20}H_{30}O_2$), Nano-Zn Oxide and Nano-rock Phosphate, in *Energy and Environment*, Springer, 2018, pp. 89–101.
10 C. J. Dedman, *et al.*, Environmentally relevant concentrations of titanium dioxide nanoparticles pose negligible risk to marine microbes, *Environ. Sci.: Nano*, 2021, **8**(5), 1236–1255.
11 N. S. Taylor, *et al.*, Molecular toxicity of cerium oxide nanoparticles to the freshwater alga Chlamydomonas reinhardtii is associated with supra-environmental exposure concentrations, *Nanotoxicology*, 2016, **10**(1), 32–41.
12 P. Yu, *et al.*, Self-assembled high-strength hydroxyapatite/graphene oxide/chitosan composite hydrogel for bone tissue engineering, *Carbohydr. Polym.*, 2017, **155**, 507–515.
13 M. Szymonowicz, *et al.*, Cytotoxicity evaluation of high-temperature annealed nanohydroxyapatite in contact with fibroblast cells, *Materials*, 2017, **10**(6), 590.
14 T. J. Park, K. G. Lee and S. Y. Lee, Advances in microbial biosynthesis of metal nanoparticles, *Appl. Microbiol. Biotechnol.*, 2016, **100**(2), 521–534.
15 A. D. Servin and J. C. White, Nanotechnology in agriculture: next steps for understanding engineered nanoparticle exposure and risk, *NanoImpact*, 2016, **1**, 9–12.
16 N. Mitter and K. Hussey, Moving policy and regulation forward for nanotechnology applications in agriculture, *Nat. Nanotechnol.*, 2019, **14**(6), 508–510.
17 A. Priyam, *et al.*, A new method for biological synthesis of agriculturally relevant nanohydroxyapatite with elucidated effects on soil bacteria, *Sci. Rep.*, 2019, **9**(1), 1–14.
18 A. Priyam, *et al.*, Abiotic factors and aging alter the physicochemical characteristics and toxicity of Phosphorus nanomaterials to zebrafish embryos, *NanoImpact*, 2022, **25**, 100387.
19 K. E. Wheeler, *et al.*, Environmental dimensions of the protein corona, *Nat. Nanotechnol.*, 2021, **16**(6), 617–629.
20 B. Neun, A. Ilinskaya and M. Dobrovolskaia, Analysis of hemolytic properties of nanoparticles, *NCL Method ITA-1 Version 1.2*, Nanotechnology Characterization Laboratory, Frederick, MD, 2016.
21 A. K. Teotia, *et al.*, Nano-hydroxyapatite bone substitute functionalized with bone active molecules for enhanced cranial bone regeneration, *ACS Appl. Mater. Interfaces*, 2017, **9**(8), 6816–6828.
22 A. K. Teotia, I. Qayoom and A. Kumar, Endogenous Platelet-Rich Plasma Supplements/Augments Growth Factors Delivered via Porous Collagen-Nanohydroxyapatite Bone Substitute for Enhanced Bone Formation, *ACS Biomater. Sci. Eng.*, 2018, **5**(1), 56–69.
23 Q. Wang, *et al.*, Controlled dual delivery of low doses of BMP-2 and VEGF in a silk fibroin–nanohydroxyapatite scaffold for vascularized bone regeneration, *J. Mater. Chem. B*, 2017, **5**(33), 6963–6972.
24 B. Yilmaz, S. Doğan and S. Ç. Kasimoğullari, Hemocompatibility, cytotoxicity, and genotoxicity of poly (methylmethacrylate)/nanohydroxyapatite nanocomposites synthesized by melt blending method, *Int. J. Polym. Mater. Polym. Biomater.*, 2018, **67**(6), 351–360.
25 L. Wang, *et al.*, Cytotoxicity and hemolytic properties of nano-hydroxyapatite/polyetheretherketone biocomposites, in *Materials Science Forum*, Trans Tech Publ, 2016.
26 V. P. Padmanabhan, *et al.*, Advanced lithium substituted hydroxyapatite nanoparticles for antimicrobial and hemolytic studies, *New J. Chem.*, 2019, **43**(47), 18484–18494.
27 G. Moore, M. Ledford and A. Merydith, A micromodification of the Drabkin hemoglobin assay for measuring plasma hemoglobin in the range of 5 to 2000 mg/dl, *Biochem. Med.*, 1981, **26**(2), 167–173.

© 2023 The Author(s). Published by the Royal Society of Chemistry

Open Access Article. Published on 20 prosince 2022. Downloaded on 27.01.2026 16:22:53.
This article is licensed under a Creative Commons Attribution-NonCommercial 3.0 Unported Licence.

28 N. Shida, *et al.*, Study of plasma coagulation induced by contact with calcium chloride solution, *Soft Matter*, 2016, **12**(47), 9471–9476.
29 M.-C. Wang, G. D. Pins and F. H. Silver, Preparation of fibrin glue: the effects of calcium chloride and sodium chloride, *Mater. Sci. Eng., C*, 1995, **3**(2), 131–135.
30 N. J. Kruger, The Bradford method for protein quantitation, in *The Protein Protocols Handbook*, Springer, 2009, pp. 17–24.
31 A. Tsatsakis, *et al.*, In vitro blood compatibility and in vitro cytotoxicity of amphiphilic poly-N-vinylpyrrolidone nanoparticles, *Food Chem. Toxicol.*, 2019, **127**, 42–52.
32 S. Deb, *et al.*, Surface tunability of nanoparticles in modulating platelet functions, *Blood Cells, Mol., Dis.*, 2012, **48**(1), 36–44.
33 H. Huang, *et al.*, An evaluation of blood compatibility of silver nanoparticles, *Sci. Rep.*, 2016, **6**(1), 1–15.
34 V. K. Sharma, *et al.*, Interactions between silver nanoparticles and other metal nanoparticles under environmentally relevant conditions: a review, *Sci. Total Environ.*, 2019, **653**, 1042–1051.
35 N. I. Supiandi, *et al.*, Isotopically Labeled Nanoparticles at Relevant Concentrations: How Low Can We Go? The Case of CdSe/ZnS QDs in Surface Waters, *Environ. Sci. Technol.*, 2019, **53**(5), 2586–2594.
36 P. A. Holden, *et al.*, Evaluation of exposure concentrations used in assessing manufactured nanomaterial environmental hazards: are they relevant?, *Environ. Sci. Technol.*, 2014, **48**(18), 10541–10551.
37 J. Zhao, *et al.*, Engineered nanomaterials in the environment: are they safe?, *Crit. Rev. Environ. Sci. Technol.*, 2020, 1–36.
38 J. Zhu, *et al.*, Toxicological evaluation of ionic liquid in a biological functional tissue construct model based on nano-hydroxyapatite/chitosan/gelatin hybrid scaffolds, *Int. J. Biol. Macromol.*, 2020, **158**, 800–810.
39 H. Yang, *et al.*, In vitro evaluation of a novel multiwalled carbon nanotube/nanohydroxyapatite/polycaprolactone composite for bone tissue engineering, *J. Mater. Res.*, 2019, **34**(4), 532–544.
40 M. Gao, *et al.*, Oxidative stress and DNA damage in zebrafish liver due to hydroxyapatite nanoparticles-loaded cadmium, *Chemosphere*, 2018, **202**, 498–505.
41 M. Gao, *et al.*, Toxic effects of nanomaterial-adsorbed cadmium on Daphnia magna, *Ecotoxicol. Environ. Saf.*, 2018, **148**, 261–268.
42 J. Simak and S. De Paoli, The effects of nanomaterials on blood coagulation in hemostasis and thrombosis, *Wiley Interdiscip. Rev.: Nanomed. Nanobiotechnol.*, 2017, **9**(5), e1448.
43 S. Abbina, *et al.*, Blood circulation of soft nanomaterials is governed by dynamic remodeling of protein opsonins at nano-biointerface, *Nat. Commun.*, 2020, **11**(1), 1–12.
44 S. Pokhrel, Hydroxyapatite: preparation, properties and its biomedical applications, *Adv. Chem. Eng. Sci.*, 2018, **8**(04), 225.
45 K. Pajor, L. Pajchel and J. Kolmas, Hydroxyapatite and fluorapatite in conservative dentistry and oral implantology—a review, *Materials*, 2019, **12**(17), 2683.
46 N. Kottegoda, *et al.*, Urea-hydroxyapatite nanohybrids for slow release of nitrogen, *ACS Nano*, 2017, **11**(2), 1214–1221.
47 N. Madusanka, *et al.*, Urea–hydroxyapatite-montmorillonite nanohybrid composites as slow release nitrogen compositions, *Appl. Clay Sci.*, 2017, **150**, 303–308.
48 Y. Bian, *et al.*, Silver nanoparticles promote procoagulant activity of red blood cells: a potential risk of thrombosis in susceptible population, *Part. Fibre Toxicol.*, 2019, **16**(1), 1–14.
49 E. P. Babu, *et al.*, Size dependent uptake and hemolytic effect of zinc oxide nanoparticles on erythrocytes and biomedical potential of ZnO-ferulic acid conjugates, *Sci. Rep.*, 2017, **7**(1), 1–12.
50 T. Surendra, *et al.*, Vegetable peel waste for the production of ZnO nanoparticles and its toxicological efficiency, antifungal, hemolytic, and antibacterial activities, *Nanoscale Res. Lett.*, 2016, **11**(1), 546.
51 N. L. Martínez-Rodríguez, S. Tavárez and Z. I. González-Sánchez, In vitro toxicity assessment of zinc and nickel ferrite nanoparticles in human erythrocytes and peripheral blood mononuclear cell, *Toxicol. In Vitro*, 2019, **57**, 54–61.
52 A. Ouidad, C. Sara and D. Samir, Biological properties and Acute Toxicity Study of Copper oxide nanoparticles prepared by aqueous leaves extract of Portulaca oleracea (L), *Asian J. Pharm. Res.*, 2020, **10**(2), 89–94.
53 C. Santos, *et al.*, Vascular biosafety of commercial hydroxyapatite particles: discrepancy between blood compatibility assays and endothelial cell behavior, *J. Nanobiotechnology*, 2018, **16**(1), 1–15.
54 C.-H. Ooi, *et al.*, Physicochemical evaluation and in vitro hemocompatibility study on nanoporous hydroxyapatite, *J. Mater. Sci.: Mater. Med.*, 2019, **30**(4), 44.
55 M. S. Laranjeira, *et al.*, Different hydroxyapatite magnetic nanoparticles for medical imaging: its effects on hemostatic, hemolytic activity and cellular cytotoxicity, *Colloids Surf., B*, 2016, **146**, 363–374.
56 S.-H. Yun, *et al.*, Platelet activation: the mechanisms and potential biomarkers, *BioMed Res. Int.*, 2016, **2016**, 9060143.
57 D. R. Riddell and J. S. Owen, Inhibition of ADP-induced platelet aggregation by apoE is not mediated by membrane cholesterol depletion, *Thromb. Res.*, 1996, **81**(5), 597–606.
58 D. R. Riddell, A. Graham and J. S. Owen, Apolipoprotein E inhibits platelet aggregation through the l-arginine: nitric oxide pathway implications for vascular disease, *J. Biol. Chem.*, 1997, **272**(1), 89–95.
59 T. Chavakis, *et al.*, Inhibition of platelet adhesion and aggregation by a defined region (Gly-486–Lys-502) of high molecular weight kininogen, *J. Biol. Chem.*, 2002, **277**(26), 23157–23164.
60 B. Kharazian, N. Hadipour and M. Ejtehadi, Understanding the nanoparticle–protein corona complexes using computational and experimental methods, *Int. J. Biochem. Cell Biol.*, 2016, **75**, 162–174.

61 S. T. Yang, *et al.*, Biosafety and bioapplication of nanomaterials by designing protein–nanoparticle interactions, *Small*, 2013, **9**(9–10), 1635–1653.
62 Y. K. Lee, *et al.*, Effect of the protein corona on nanoparticles for modulating cytotoxicity and immunotoxicity, *Int. J. Nanomedicine*, 2015, **10**, 97.
63 V. H. Nguyen and B.-J. Lee, Protein corona: a new approach for nanomedicine design, *Int. J. Nanomedicine*, 2017, **12**, 3137.

Open Access Article. Published on 20 prosince 2022. Downloaded on 27.01.2026 16:22:53.
This article is licensed under a Creative Commons Attribution-NonCommercial 3.0 Unported Licence.

© 2023 The Author(s). Published by the Royal Society of Chemistry